ARTICLE

Effects of Activation Atmospheres on Structure and Activity of Mo-based Catalyst for Synthesis of Higher Alcohols

Ji-long Zhou[a], Wei Xie[a], Song Sun[a]*, Li-li Ji[a], Li-rong Zheng[b], Chen Gao[a,c], Jun Bao[a,c]*

a. National Synchrotron Radiation Laboratory, Collaborative Innovation Center of Chemistry for Energy Materials, University of Science and Technology of China, Hefei 230029, China
b. Institute of High Energy Physics, Chinese Academy of Science, Beijing 100039, China
c. CAS Key Laboratory of Materials for Energy Conversion, Department of Materials Science and Engineering, University of Science and Technology of China, Hefei 230026, China

(Dated: Received on March 2, 2016; Accepted on April 12, 2016)

Activated carbon supported Mo-based catalysts were prepared and reduced under different activation atmospheres, including pure H_2, syngas (H_2/CO=2/1), and pure CO. The catalysts structures were characterized by X-ray diffraction , X-ray absorption fine structure, and *in situ* diffuse reflectance infrared Fourier transform spectroscopy. The catalytic performance for the higher alcohol synthesis from syngas was tested. The pure H_2 treatment showed a high reduction capacity. The presence of a large amount of metallic Co^0 and low valence state $Mo^{\varphi+}$ ($0<\varphi<2$) on the surface suggested a super activity for the CO dissociation and hydrogenation, which promoted hydrocarbons formation and reduced the alcohol selectivity. In contrast, the pure CO-reduced catalyst had a low reduction degree. The Mo and Co species at the catalyst mainly existed in the form of Mo^{4+} and Co^{2+}. The syngas-reduced catalyst showed the highest activity and selectivity for the higher alcohols synthesis. We suggest that the syngas treatment had an appropriate reduction capacity that is between those of pure H_2 and pure CO and led to the coexistence of multivalent Co species as well as the enrichment of $Mo^{\delta+}$ on the catalyst's surface. The synergistic effects between these active species provided a better cooperativity and equilibrium between the CO dissociation, hydrogenation and CO insertion and thus contributed beneficially to the formation of higher alcohols.

Key words: Higher alcohol synthesis, Activation mechanism, *in situ* diffuse reflectance infrared Fourier transform spectroscopy, Mo-based catalyst, Syngas

I. INTRODUCTION

Higher alcohols (C_{2+} alcohols) are alternative additives for the improvement of the octane number in gasoline and can also be used as clean fuels and petrochemical feed stocks. Consequently, the higher alcohols synthesis (HAS) from syngas derived from coal, biomass, and natural gas has attracted significant attention because of the scarcity of energy resources, environmental concerns and gasoline additive octane demands. Therefore, several catalytic systems have been developed for this reaction since the last decades. Among them, the alkali metal promoted Mo-based catalyst is regarded as one of the most promising candidates due to the excellent resistance to sulfur poisoning [1−6]. Furthermore, the incorporation of Co or Ni promoters can improve the alcohol selectivity and space-time-yield (STY), especially for the growth of the carbon chain [7]. In the case of the MoS_2-based catalyst, the synergy between Co and MoS_2 species played an important role in the catalytic performance. Indeed, the "Co-Mo-S" phase was suggested to be responsible for the alcohol synthesis [8]. Similarly, in the case of reduced Mo-based catalysts, the strong interaction between Co and Mo species was conducive to the formation of higher alcohols [9, 10].

In general, the activation of the catalyst is a necessary step for the determination of the catalytic activity. The activation process plays a crucial role in the performance of the reaction as the catalyst's structure undergoes an extensive reconstruction during this process in order to form the catalytic species [11]. A Fischer-Tropsch (FT) catalyst has been paid attention to. Bian *et al.* [12] studied the activation of Fe catalyst in different reducing atmospheres. The H_2-reduced sample had a strong interaction between the adsorbed CO and Fe carbides while the interaction was rather weak for syngas- and CO-reduced samples. The fine Fe carbide particles formed during the reduction in syngas or in CO played an important role in morphological reactions of the Fe catalyst during the FT synthesis. In the case of

*Authors to whom correspondence should be addressed. E-mail: baoj@ustc.edu.cn, suns@ustc.edu.cn

the SBA-15 supported Fe catalyst [13], the different activation treatments led to different Fe species in fresh catalysts: α-Fe, Fe_3O_4, and Fe^{2+} diffused into the SBA-15 walls with H_2-reduced Fe/SBA-15 and χ-Fe_5C_2, Fe_3O_4 and Fe^{2+} with syngas-reduced Fe/SBA-15. The H_2-reduced catalyst exhibited a higher activity for CO hydrogenation. The study on a CoCu catalyst [14] for higher alcohol synthesis revealed that the CO-activated catalyst showed significantly higher activity and Anderson−Schulz−Flory chain lengthening probability, but relatively lower alcohol selectivity compared to the same catalyst activated by H_2 or syngas. The results of the characterization indicated that an "onion-like" graphitic carbon shell was observed for the CO-activated Co_2Cu_1 catalyst. The syngas and CO activation led to higher Co/Cu ratio compared to nominal Co/Cu surface ratio. So far, very few studies have focused on the activation of Mo catalysts. Sun *et al.* [15] reported that pretreatment of the sulfided K_2CO_3/MoS_2 catalyst could remarkably shorten the time of induction period as well as promote the catalytic activity. The higher alcohols content were enhanced after pretreatment of the catalyst by CO or syngas. To the best of our knowledge, no research has been done on the activation of oxidation state of a Mo-based catalyst. We have previously developed a specific K-Co-Mo catalyst with excellent performance for the higher alcohol synthesis. Base on the above analyses, in this work, we systematically study on the activation of the K-Co-Mo catalyst. The syngas, H_2, and CO were used as reduction gases to activate the catalyst. The catalyst structure and CO adsorption properties were characterized by X-ray diffraction (XRD), X-ray absorption fine structure (XAFS), and *in situ* diffuse reflectance infrared Fourier transform spectroscopy (DRIFTS), and the catalytic performance for the higher alcohols synthesis was investigated. We discuss the relationship between the structure and catalytic performance.

II. EXPERIMENTS

A. Catalyst preparation

The activated-carbon-supported K-Co-Mo catalysts (K-Co-Mo/AC) were prepared via a sol-gel method combined with pore volume impregnation as described in our previous studies [16, 17]. A typical procedure is as follows: firstly the Co $(NO_3)_2$ (AR) aqueous solution, citric acid (AR) aqueous solution and K_2CO_3 (AR) aqueous solution were prepared and slowly added to $(NH_4)_6Mo_7O_{24}{\cdot}6H_2O$ (AR) solution under continuous stirring. Then the pH value of the mixed solution was adjusted to 3.5 by addition of HCOOH or NH_4OH. The mixed solution was kept in a water bath at 343 K for about 6 h to form the K-Co-Mo sol. Finally the as-prepared sol was then impregnated into activated carbon. After ultrasonic dispersion for 5 min, the mixture was dried at 393 K overnight and calcined in flowing nitrogen at 673 K for 4 h. The activated carbons, with the size of 10−20 mesh, was supplied by Fujian Xin Sen Carbon Co. Ltd. Prior to use, the support was first washed using 30% nitric acid solution at room temperature overnight, followed by thorough washing with deionized water and drying in air at 393 K overnight and then flushing with nitrogen (99.999%) at 453 K for 2 h to remove any surface adsorbates. The Mo content in the as-prepared catalysts, expressed as the weight ratio Mo/AC, was kept constant at 40 wt%. The atomic ratios of K/Mo and Co/Mo were 0.1 and 0.5, respectively.

B. Catalyst characterization

Powder XRD patterns were recorded with a RigaKu D/max-γA rotating-anode diffractometer (RigaKu Corp., Japan) using Cu-Kα radiation source (40 kV and 200 mA). The scan range (2θ) was from 10° to 70°.

The X-ray absorption spectra at the Mo and Co K-edge of the catalysts and standard compounds were recorded at the 1W1B beamline of the Beijing Synchrotron Radiation Facility (BSRF, China). The storage ring energy was operated at 2.5 GeV with a typical current of 250 mA. The energy calibration of the Mo and Co K-edge was calibrated using Mo and Co foil, respectively. All samples were ground into fine powder and brushed onto adhesive tapes. Data processing and analysis were performed using a standard procedure.

The adsorption of CO on the surface of catalysts was studied by *in situ* DRIFTS using a Bruker Vertex 70v FT-IR spectrometer (Bruker Ltd., Germany) equipped with a MCT detector, a DRIFTS accessory and a reaction cell (Harrick Scientific Products Inc., USA). Prior to the start of the experiment, the catalysts were pre-reduced for 12 h at 623 K. After cooling down to room temperature, the reduced catalyst was passivated in a flow of a $1\%O_2/N_2$ gas mixture (40 mL/min) for 2 h. The passivated catalyst (15 mg) was placed in the sample cup covered by a dome equipped with CaF_2 windows and then further reduced *in situ* for 90 min under the same condition as used in the pre-reduction step. After reduction, the feed gas was switched to pure N_2 (40 mL/min) and applied for 1 h. The system was then cooled down to 298 K and the background spectra were recorded. CO adsorption was carried out at 298 K by introducing pure CO to the reaction cell at a rate of 10 mL/min for 30 min. Infrared spectra were recorded in reflectance mode between 600 and 4000 cm^{-1} with 32 scans, a resolution of 4 cm^{-1} and at a scan velocity of 20 kHz.

C. Catalytic activity measurements

The catalytic activity measurements were carried out in a tubular fixed-bed reactor with an inner diameter of 8 mm. For each experiment, 0.5 g of the catalyst

DOI:10.1063/1674-0068/29/cjcp1603038

(size between 10 and 20 mesh) were diluted with quartz sand to obtain a total volume of 2 mL. Prior to the reaction, the catalyst was reduced in a flow of a reducing gas (40 mL/min) for 12 h. The reducing gas was either pure H_2, syngas (60%H_2, 30%CO, and 10%N_2) or pure CO. The temperature of the reduction step was programmed to rise from room temperature to a target temperature, which was maintained for 12 h, and then to reduce the temperature down to the reaction temperature of 333 K at which the reactor was fed with syngas containing 60%H_2, 30%CO, and 10%N_2. The product gas was cooled down to 273 K in a trap surrounded by ice-water and separated into gas and liquid phases at the reaction pressure. Details on the product analytical procedure are described in our previous work [17]. All the activity measurements were performed under the reaction condition of 5.0 MPa, 623 K, and gas hourly space velocity (GHSV) 2400 h^{-1}. The activity data in this study were analyzed 24 h after the reaction start because the alcohol synthesis required an induction period.

III. RESULTS AND DISCUSSION

A. XRD Results

The XRD patterns of the K-Co-Mo/AC catalysts reduced by different reducing atmosphere are shown in Fig.1. For comparison, the XRD patterns of the fresh unsupported and supported K-Co-Mo samples are also presented. The unsupported catalyst exhibited three very weak peaks at 26.1°, 37.0°, and 53.5° attributed to MoO_2. Indeed, the decomposition of citric acid present in the gel reduces Mo^{6+} species under nitrogen [16, 17]. Besides, no peaks assigned to K-Mo nor Co species were detected. The supported K-Co-Mo catalysts exhibited significantly weaker diffraction intensities than that of the unsupported catalyst. The weak and broad diffraction peak around 25.0° was assigned to the activated carbon support. After reduction under different atmospheres, almost no obvious diffraction peaks were observed in all cases. The results indicate that both the fresh and reduced K-Co-Mo/AC catalysts exhibit an amorphous structure and that the catalytic components were highly dispersed on the surface of the activated carbon.

B. XAFS results

In contrast to XRD, which can only probe structure information at a long-range order in a material, XAFS is mainly sensitive to the local surroundings of the atoms and is considered to be one of the most powerful methods for the determination of the structure of amorphous or highly dispersed catalysts. Figure 2 presents the Mo K-edge X-ray absorption near-edge structure (XANES)

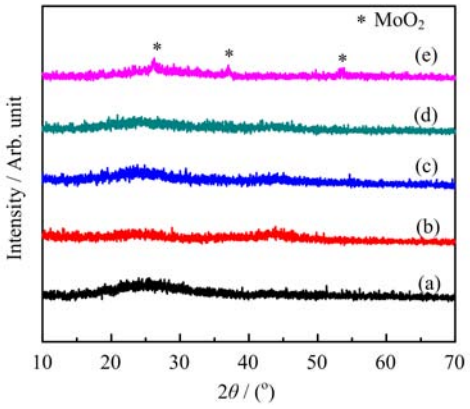

FIG. 1 XRD patterns of (a) fresh supported K-Co-Mo/AC catalyst, (b) H_2-reduced catalyst, (c) syngas-reduced catalyst, (d) CO-reduced catalyst, and (e) fresh unsupported K-Co-Mo catalyst.

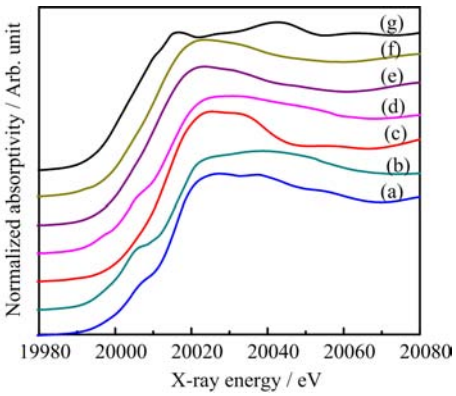

FIG. 2 Mo K-edge XANES spectra of (a) standard MoO_3, (b) fresh K-Co-Mo/AC catalyst, (c) standard MoO_2, (d) CO-reduced catalyst, (e) H_2-reduced catalyst, (f) syngas-reduced catalyst, and (g) Mo foil.

spectra of the fresh and reduced K-Co-Mo/AC catalysts, together with Mo foil, MoO_2 and MoO_3 as reference materials. The absorption edge position provides information on the chemical valence of the central metal atoms; and the pre-edge peak intensity is sensitive to the symmetry of the absorbing atom and can therefore provide structural information on the first coordination shell [18]. Compounds with a tetrahedrally coordinated absorbing atom generally exhibit an intense pre-edge peak. While in the case of octahedrally coordinated compounds, such pre-edge peak is usually weak. MoO_3 has a layered structure and each layer is composed of distorted MoO_6 octahedra that share both edges and corners. As expected, a weak pre-edge peak was observed in the XANES spectra of MoO_3 (Fig.2(a)). By contrast, MoO_2 (Fig.2(c)) has a strictly octahedral field and no obvious pre-edge peak was observed. The fresh supported K-Co-Mo/AC catalyst (Fig.2(b)) exhibited a more intense pre-edge peak than that of MoO_3, and the absorption edge shifted to a lower energy, close to that

DOI:10.1063/1674-0068/29/cjcp1603038

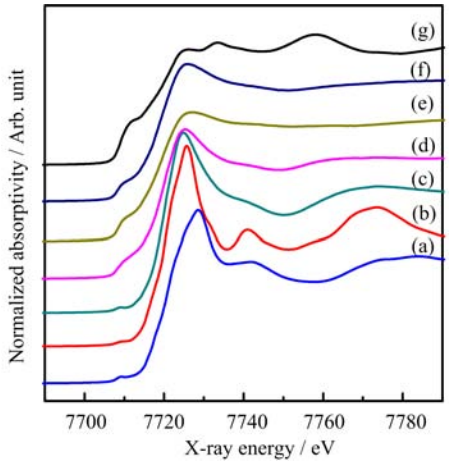

FIG. 3 Co K-edge XANES spectra of (a) standard Co_3O_4, (b) standard CoO, (c) fresh K-Co-Mo/AC catalyst, (d) H_2-reduced catalyst, (e) syngas-reduced catalyst, (f) CO-reduced catalyst, and (g) Co foil.

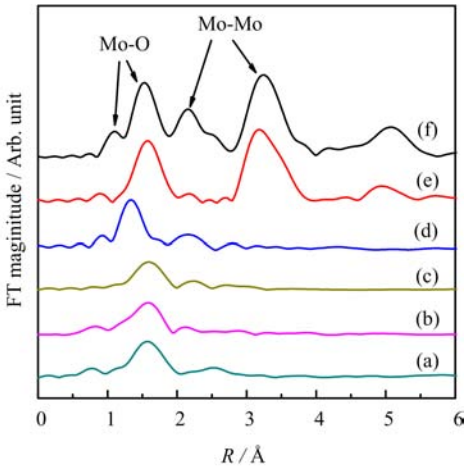

FIG. 4 Fourier transforms of Mo K-edge EXAFS of (a) H_2-reduced catalyst, (b) syngas-reduced catalyst, (c) CO-reduced catalyst, (d) fresh K-Co-Mo/AC catalyst, (e) standard MoO_3, and (f) standard MoO_2.

of MoO_2. The results imply that the Mo species in the fresh sample existed in a not only octahedral but also tetrahedral coordination. The lower absorption edge was observed due to the formation of MoO_2, which is consistent with the XRD result. For the CO-reduced catalyst, a weak pre-edge peak was observed and the absorption edge appeared close to that of MoO_2. The syngas or H_2-reduced catalysts presented no obvious pre-edge peak and their absorption edges were located between that of the standard MoO_2 and of the Mo foil. These results suggest that the CO reduction produced more Mo^{4+} species, while the syngas or H_2 reduction promoted the formation of lower valence state Mo species with an octahedral coordination.

The Co K-edge XANES spectra of the fresh K-Co-Mo/AC catalyst, the samples reduced with H_2, syngas and CO as well as the standards Co_3O_4, CoO, and CoO foil, are shown in Fig.3. The absorption edge of the Co K-edge in fresh K-Co-Mo/AC catalyst was very similar to that of the standard CoO, indicating the presence of Co^{2+} species. After reduction, the adsorption edge of Co K-edge was shifted towards a lower energy and closer to that of the Co foil. The shifting behavior of the three reduced catalysts can be ranked in the following order: H_2-reduced catalyst>syngas-reduced catalyst>CO-reduced catalyst. The pure H_2 treatment showed the strongest reducing capacity indicating that the main Co species present in the reduced catalyst was the metallic Co^0.

Figure 4 shows the Fourier transforms (FT) of the Mo K-edge EXAFS spectra of fresh and reduced K-Co-Mo/AC catalysts, together with the standard compounds MoO_2 and MoO_3. The FT of the fresh K-Co-Mo/AC catalyst (Fig.4(d)) exhibited a similar feature to that of MoO_2. This observation corroborates with the conclusion of XRD and XANES results. The reduced catalysts showed a weaker Mo-O and Mo-Mo coordination peaks as compared to that of the fresh sample, indicating that the reduction process destroyed the ordered structure of Mo species to some extent, resulting in a lower crystallization degree.

The FT of Co K-edge EXAFS spectra of the catalysts and standard materials Co_3O_4, CoO and Co foil are presented in Fig.5. The resemblance of the fresh K-Co-Mo/AC catalyst spectrum to that of the standard Co-O reveals that the Co species in the fresh catalyst were mainly under the form of CoO, which is fully consistent with the XANES results. After reduction, the intensity of the Co-O coordination peak decreased significantly, whilst an obvious Co-Co coordination appeared at a coordination distance which was the same as that of the Co foil. Overall, the H_2-reduced catalyst showed the strongest Co-Co coordination, while the weakest peak was observed for the CO-reduced sample. Combined with the XANES and EXAFS results, the H_2 reduction promoted the most formation of metallic Co^0 while for the CO-reduced sample, the Co species were mainly present under the form of Co^{2+} species.

C. *In situ* DRIFTS results

The DRIFTS spectra of CO adsorbed on the reduced catalyst by H_2, syngas and CO are shown in Fig.5. In the case of the H_2-reduced catalyst (Fig.5(a), the broad bands at 2171 and 2115 cm^{-1} were observed and are characteristic of gaseous CO [19]. The bands at 2103 cm^{-1} and 2050−2065 cm^{-1} are attributed to the linear stretching vibrations of the CO adsorbed on $Mo^{\delta+}$ ($1<\delta<4$) [7, 20, 21, 27] and $Mo^{\varphi+}$ ($0<\varphi<2$) [22], respectively. The bands at 2027 and 2038 cm^{-1} can be assigned to the CO adsorbed on metallic Co^0 [23]. The syngas-reduced sample (Fig.5(b)) exhibited three

DOI:10.1063/1674-0068/29/cjcp1603038

TABLE I Effect of reducing gas type and reduction temperature on the catalytic performance towards alcohol formation from syngas.

Gas	T/K	Co conv.%	C_nOH selectivity/%					Alc. Sel.[a]/%	Alc. STY/(g/(kg·h))	MeOH/C_{2+}OH
			MeOH	EtOH	PrOH	BuOH	PeOH			
Syngas	673	17.24	18.85	12.00	3.9	0.72	0.17	35.65	63.14	1.13
	623	24.15	17.00	16.20	6.77	1.68	0.57	42.22	101.75	0.70
	573	28.02	3.99	2.92	0.98	0.36	0.21	8.47	48.72	0.93
H_2	673	58.88	6.06	3.37	1.78	0.48	0.22	11.95	51.93	1.07
	623	38.61	11.87	9.1	4.08	0.89	0.33	26.26	87.42	0.84
	573	41.34	10.76	8.05	2.6	0.56	0.24	22.21	88.87	0.96
CO	673	10.22	15.05	11.38	4.46	1.40	0.70	32.98	18.76	0.87
	623	20.19	15.56	16.28	5.48	1.41	0.66	39.40	79.67	0.67
	573	36.50	10.13	8.40	2.79	1.51	1.54	24.37	94.10	0.80

Note: T is temperature of reduction.
[a]. Based on CO_2-free carbon atoms.

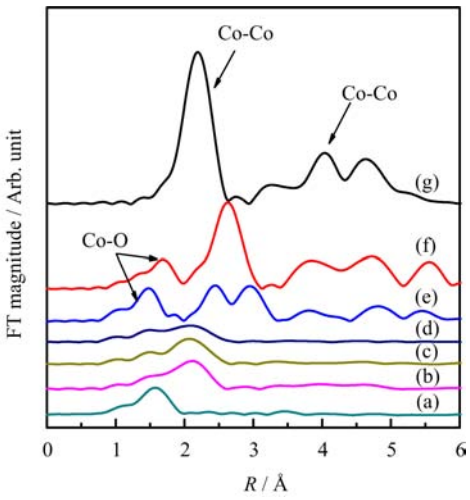

FIG. 5 Fourier transforms of Co K-edge EXAFS of (a) fresh K-Co-Mo/AC catalyst, (b) H_2-reduced catalyst, (c) syngas-reduced catalyst, (d) CO-reduced catalyst, (e) standard Co_3O_4, (f) standard CoO, and (g) Co foil.

new bands at 2075, 2126, and 2167 cm^{-1} corresponding to the bands of the CO adsorbed on Mo^{2+}, Co^{1+} and Co^{2+}, respectively [22, 23].

Furthermore, the intensity of the 2103 cm^{-1} band assigned to the CO adsorbed on $Mo^{\delta+}$ was stronger as compared to that of the H_2-reduced sample. Figure 5(c) illustrates the DRIFTS spectra of the CO adsorbed on the CO-reduced catalyst. A new band appeared at 2180 cm^{-1} and can be attributed to the CO adsorbed on $Co^{\chi+}$ ($2<\chi<3$) [23]. Besides, the bands assigned to the CO adsorbed on Co^{1+} and Co^{2+} sites became more apparent, while the band due to the CO adsorbed on Co^0 decreased significantly. The *in situ* DRIFTS results clearly indicate that the Co species on the surface of pure H_2-reduced catalyst were mainly present under the form of metallic Co^0. In the case of the CO reduced sample, most of the surface Co species still remained in the oxidized state while the ones of the syngas-reduced catalyst showed to be both metallic Co^0 and the oxidized state. The Co^0, Co^{1+} and Co^{2+} species coexisted on the catalyst surface.

D. Catalytic performance

The catalytic performance for higher alcohol synthesis with the K-Co-Mo/AC catalysts reduced by different reducing gas at different temperatures was tested and the activity data have been recorded after an induction period of 24 h (Table I). The pure H_2, syngas and CO-reduced catalysts showed similar trends when the temperature of the reduction increased. As shown in Table I, the alcohol selectivity, as well as the C_{2+}OH content in alcohol distribution, significantly increased for the three catalysts when the temperature of reduction increases from 573 K to 623 K reaching the highest level at the optimal temperature of 623 K. Increasing the temperature up to 673 K had a negative effect on the catalytic performance. The syngas-reduced catalyst showed the highest activity for alcohol synthesis: the total alcohol STY reached 101.75 g/(kg·h) with a selectivity of 42.22%, and the carbon atomic ratio of MeOH/C_{2+}OH decreased to 0.70. By contrast, the H_2-reduced sample showed the lowest catalytic activity, especially for the alcohol selectivity which was only 26.26%.

The synthesis of higher alcohols with Mo-based catalysts follows a CO insertion mechanism [24−26]. First, the adsorbed CO molecule is dissociated and then hydrogenated to form CH_2. The alkyl chain grows via a CH_2 insertion. In a second step, the non-dissociation of adsorbed CO molecules insert alkyl groups to form acyl species, which can be further hydrogenated to form the alcohol product or a longer alkyl group by hydrogenation. According to the mechanism, the alkyl group

DOI:10.1063/1674-0068/29/cjcp1603038

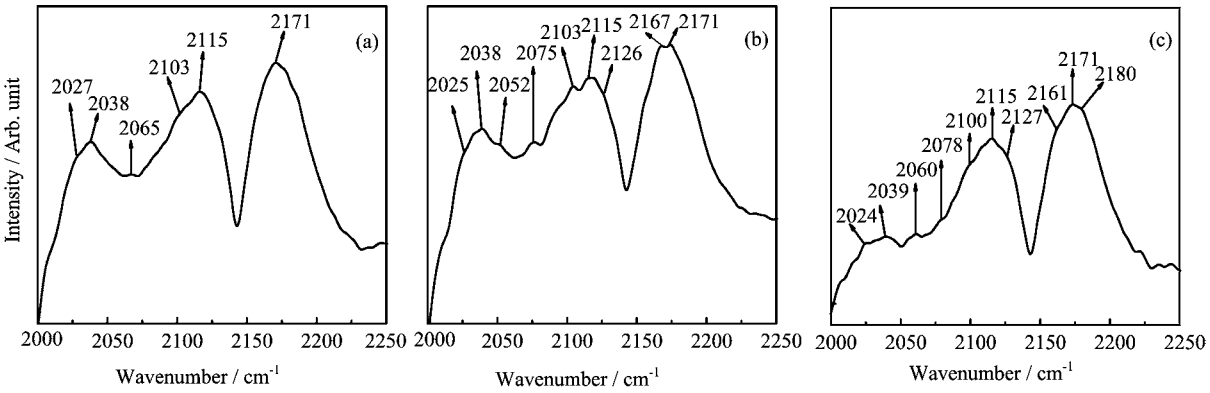

FIG. 6 *In situ* DRIFTS of CO adsorption on (a) H_2-reduced catalyst, (b) syngas-reduced catalyst, and (c) CO-reduced catalyst.

is regarded as the key intermediate for higher alcohols synthesis. This complex nature of the reaction requires synergy between different active species with different functionalities, which each plays a vital role in the catalytic activity. A good catalyst for the synthesis of higher alcohols should possess an excellent cooperativity between the reaction of CO dissociation, hydrogenation and CO insertion. Too strong capabilities for the CO dissociation or hydrogenation can favor the hydrogenation of alkyl group to form hydrocarbons and thus inhibit the alcohol synthesis. If the catalyst has a too weak capability, the total conversion of CO is low.

Activated Mo-based catalysts are known to exhibit at their surface $Mo^{\delta+}$ ($1<\delta<4$) species which are responsible for the CO adsorption and thus alcohol formation [24, 27]. Further studies by Li *et al.* [28] suggested that the Mo species with an average valence state of +3.5 are active for the alcohol formation from syngas. The reason can be attributed to the fact that the $Mo^{\delta+}$ ($1<\delta<4$) species are favorable adsorption sites for the non-dissociative CO and favor the CO insertion into alkyl species to produce alcohol. Co is an effective promoter for Mo-based catalysts in order to enhance the alcohol production, especially the C_{2+} alcohol formation, because of the formation of intermediate alkyl groups [29−31]. It is known that each Co moiety plays a different role in the reaction. Specifically, metallic Co^0 is highly active for the CO dissociative adsorption and hydrogenation, which is widely considered to be the active center of the Fischer-Tropsch reaction for hydrocarbons formation. The Co^{2+} and $Co^{\gamma+}$ ($0<\gamma<2$) species are regarded as the adsorption sites for non-dissociative CO. Tokunaga *et al.* [32] studied the alkali metal-modified Co catalysts, which worked efficiently in the Fischer-Tropsch synthesis to produce higher alcohols. They suggested that the Co^{2+} species resulted from the decrease reducibility of Co_3O_4 which were the active site for the CO insertion. Similar results were also confirmed by other researchers [33−36]. Furthermore, Smith *et al.* [37] studied the CO adsorption behavior on Cu/SiO_2, Co/SiO_2, and $CuCo/SiO_2$ catalysts using *in situ* DRIFTS. They found that the $Co^{\gamma+}$ sites favored high oxygenate yields and Co^0 site contributed to the high hydrocarbon selectivity. The results suggested that an appropriate ratio of the different active species on the catalyst surface is very important to achieve a high activity.

In our study, the characterization analysis of the different reducing atmospheres resulted in different species distributions on the catalyst. The pure H_2 treatment showed the strongest reduction capacity with the formation of $Mo^{\delta+}$ and of lower valence state $Mo^{\varphi+}$ species but mainly Co species were present under the metallic form Co^0. These results suggest that the H_2-reduced catalyst possessed relatively high activities for the CO dissociation and hydrogenation but lower CO insertion capacity favoring the hydrogenation of alkyl groups to form hydrocarbons instead of alcohols (Table I). In the case of the CO-reduced catalyst, the main species present were Mo^{4+} and Co^{2+}, which indicate a quite weak activity for the CO dissociation and hydrogenation. Consequently, the formation of the intermediate alkyl group was suppressed and ultimately decreased the alcohol production. The syngas-reduced catalyst showed the highest catalytic activity for the synthesis of higher alcohols. The reason can be attributed to the appropriate coexistence of Co^0, Co^{1+} and Co^{2+} species as well as the enrichment of $Mo^{\delta+}$ species on the surface of the catalyst due to the reduction capacity of syngas which falls in between that of pure H_2 and CO. The presence of these active species and their synergistic effects contributed to the synthesis of higher alcohol because it provided a better cooperativity between the CO dissociation, hydrogenation and CO insertion. We therefore provided new insights into the activation mechanism of Mo-based catalysts for the synthesis of higher alcohols. Furthermore, we suggest that the reduction capacity of syngas can be tuned by regulating the H_2/CO ratio, providing a potential pathway to optimize the distribution of active species and further improve the catalytic activity for the higher alcohols synthesis.

DOI:10.1063/1674-0068/29/cjcp1603038

IV. CONCLUSION

This work aimed at a systematic study on the activation of a Mo-based catalyst for the synthesis of higher alcohol, which has rarely been reported previously. Three kinds of reducing atmospheres, including pure H_2, syngas (H_2/CO=2/1), and pure CO, were employed to activate the catalysts. The different reducing atmospheres applied on a K-Co-Mo/AC catalyst led to different distributions of active species, thus exerting a significant impact on the catalytic performance. The syngas-reduced catalyst showed the highest activity for the synthesis of higher alcohols. The reason is attributed to the facts that the syngas treatment had an appropriate reduction capacity and produced a large amount of $Mo^{\delta+}$ species and multivalent state Co species on the surface of the catalyst. Their synergistic effects enhanced the cooperativity and equilibrium between the CO dissociation, hydrogenation and CO insertion and thus promoted the formation of higher alcohols. The reduction capacity of the pure CO treatment was rather weak as the main Mo and Co species in the catalyst were present under the form of Mo^{4+} and Co^{2+}. The pure H_2-reduced catalyst showed a high reduction degree. A large amount of metallic Co^0 and low valence state $Mo^{\varphi+}$ ($0<\varphi<2$) species existed in the reduced catalyst, which favored a super activity for CO dissociation and hydrogenation unfavorable to the alcohol formation.

V. ACKNOWLEDGMENTS

This work was supported by the National Natural Science Foundation of China (No.11179034 and No.11205159), the National Basic Research Program of China (No.2012CB922004).

[1] J. M. Christensen, P. A. Jensen, and A. D. Jensen, Ind. Eng. Chem. Res. **50**, 7949 (2011).
[2] J. Iranmahboob, H. Toghiani, D. O. Hill, and F. Nadim, Fuel Process Technol. **79**, 71 (2002).
[3] H. Shou, D. Ferrari, D. G. Barton, C. W. Jones, and R. J. Davis, Acs Catal. **2**, 1408 (2012).
[4] V. R. Surisetty, A. Tavasoli, and A. K. Dalai, Appl. Catal. A **365**, 243 (2009).
[5] T. Tatsumi, A. Muramatsu, T. Fukunaga, H. O. Tominaga, Polyhedron **5**, 257 (1986).
[6] S. Zaman and K. J. Smith, Catal. Rev. **54**, 41 (2012).
[7] V. R. Surisetty, A. K. Dalai, and J. Kozinski, Appl. Catal. A **385**, 153 (2010).
[8] Z. R. Li, Y. L. Fu, J. Bao, M. Jiang, T. Hu, T. Liu, and Y. N. Xie, Appl. Catal. A **220**, 21 (2001).
[9] K. Fujimoto and T. Oba, Appl. Catal. **13**, 289 (1985).
[10] D. A. Storm, Top Catal. **2**, 91 (1995).
[11] X. Cui, J. Xu, C. Zhang, Y. Yang, P. Gao, B. Wu, and Y. Li, J Catal, **282**, 35 (2011).
[12] G. Bian, A. Oonuki, Y. Kobayashi, N. Koizumi, and M. Yamada, Appl. Catal. A **219**, 13 (2001).
[13] L. A. Cano, M. V. Cagnoli, J. F. Bengoa, A. M. Alvarez, and S. G. Marchetti, J. Catal. **278**, 310 (2011).
[14] Y. Xiang, R. Barbosa, and N. Kruse, Acs Catal. **4**, 2792 (2014).
[15] H. Xiao, D. Li, W. Li, and Y. Sun, Fuel Process Technol. **91** 383 (2010).
[16] J. Bao, Y. L. Fu, and G. Z. Bian, Catal. Lett. **121**, 151 (2008).
[17] M. Lv, W. Xie, S. Sun, G. Wu, L. Zheng, S. Chu, C. Gao, and J. Bao, Catal. Sci. Technol. **5**, 2925 (2015).
[18] S. Imamura, H. Sasaki, M. Shono, and H. Kanai, J. Catal. **177**, 72 (1998).
[19] D. Song, J. Li, and Q. Cai, J. Phys. Chem. C **111**, 18970 (2007).
[20] M. I. Zaki, B. Vielhaber, and H. Knoezinger, J. Phys. Chem. **90**, 3176 (1986).
[21] J. B. Peri, J. Phys. Chem. **86**, 1615 (1982).
[22] W. Wu, Z. Wu, C. Liang, X. Chen, P. Ying, and C. Li, J. Phys. Chem. B **107**, 7088 (2003).
[23] A. Y. Khodakov, J. Lynch, D. Bazin, B. Rebours, N. Zanier, B. Moisson, and P. Chaumette, J. Catal. **168**, 16 (1997).
[24] A. Muramatsu, T. Tatsumi, and H. Tominaga, J. Phys. Chem. **96** 1334 (1992).
[25] V. Subramani and S. K. Gangwal, Energ. Fuel. **22**, 814 (2008).
[26] K. Xiao, Z. H. Bao, X. Z. Qi, X. X. Wang, L. S. Zhong, K. G. Fang, M. G. Lin, and Y. H. Sun, Chin. J. Catal. **34**, 116 (2013).
[27] M. Zhang, W. Zhang, W. Xie, Z. Qi, G. Wu, M. Lv, S. Sun, and J. Bao, J. Mol. Catal. A **395**, 269 (2014).
[28] X. G. Li, L. J. Feng, L. J. Zhang, D. B. Dadyburjor, and E. L. Kugler, Molecules **8**, 13 (2003).
[29] A. Y. Khodakov, W. Chu, and P. Fongarland, Chem. Rev. **107** 1692 (2007).
[30] N. Kruse, J. Schweicher, A. Bundhoo, A. Frennet, and T. Visart de Bocarmé, Top Catal. **48**, 145 (2008).
[31] M. Xiang, D. Li, W. Li, B. Zhong, and Y. Sun, Catal. Commun. **8**, 503 (2007).
[32] T. Ishida, T. Yanagihara, X.H. Liu, H. Ohashi, A. Hamasaki, T. Honma, H. Oji, T. Yokoyama, and M. Tokunaga, Appl. Catal. A **458**, 145 (2013).
[33] G. Jiao, Y. Ding, H. Zhu, X. Li, J. Li, R. Lin, W. Dong, L. Gong, Y. Pei, and Y. Lu, Appl. Catal. A **364** 137 (2009).
[34] G. Liu, D. Pan, T. Niu, A. Cao, Y. Yue, and Y. Liu, RSC Adv. **5**, 31637 (2015).
[35] Y. P. Pei, J. X. Liu, Y. H. Zhao, Y. J. Ding, T. Liu, W. D. Dong, H. J. Zhu, H. Y. Su, L. Yan, J. L. Li, and W. X. Li, Acs Catal. **5**, 3620 (2015).
[36] X. M. Wu, Y. Y. Guo, J. M. Zhou, G. D. Lin, X. Dong, and H. B. Zhang, Appl. Catal. A **340**, 87 (2008).
[37] M. L. Smith, N. Kumar, and J. J. Spivey, J. Phys. Chem. C **116**, 7931 (2012).

DOI:10.1063/1674-0068/29/cjcp1603038